






RESEARCH ARTICLE | AUGUST 01 2023

Demonstration of the plasmonic THz phase shifter at room temperature

K. R. Dzhekirba ; A. Shuvaev ; D. Khudaiberdiev ; I. V. Kukushkin; V. M. Muravev  

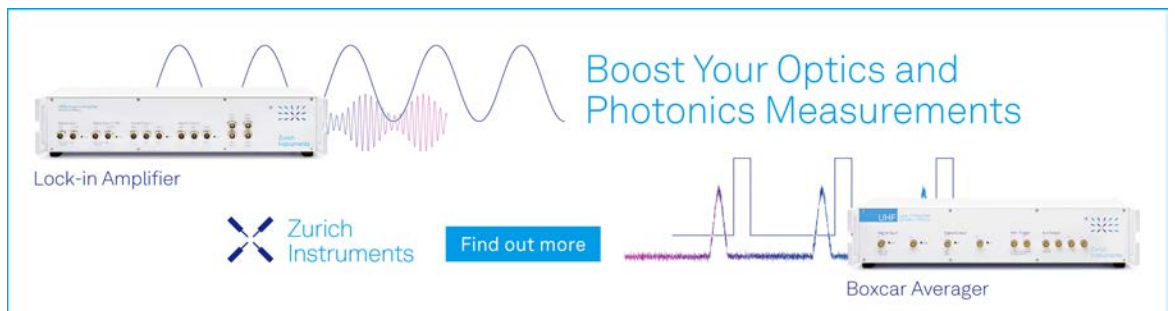


Appl. Phys. Lett. 123, 052104 (2023)

<https://doi.org/10.1063/5.0160612>



CrossMark



Boost Your Optics and Photonics Measurements

Lock-in Amplifier

Zurich Instruments

Find out more

Boxcar Averager

Demonstration of the plasmonic THz phase shifter at room temperature

Cite as: Appl. Phys. Lett. **123**, 052104 (2023); doi: [10.1063/5.0160612](https://doi.org/10.1063/5.0160612)

Submitted: 3 June 2023 · Accepted: 17 July 2023 ·

Published Online: 1 August 2023



K. R. Dzhikirba,¹ A. Shuvaev,² D. Khudaiberdiev,² I. V. Kukushkin,¹ and V. M. Muravev^{1,a)}

AFFILIATIONS

¹Institute of Solid State Physics, RAS, Chernogolovka 142432, Russia

²Institute of Solid State Physics, Vienna University of Technology, 1040 Vienna, Austria

^{a)}Author to whom correspondence should be addressed: muravev@issp.ac.ru

ABSTRACT

We experimentally demonstrate that above 300 GHz, the plasmonic phase shifter can operate at up to room temperature. We investigate the temperature-dependent behavior of the phase shift introduced by a two-dimensional electron system in a GaAs/AlGaAs heterostructure. We find that the temperature-effected changes in the relaxation time and effective mass contribute most to the phase shifter performance. The physical model developed in the study shows good agreement with the experimental data. The results open up the prospects for the practical applications of plasmonics in the terahertz frequency gap.

Published under an exclusive license by AIP Publishing. <https://doi.org/10.1063/5.0160612>

Over the years, 2D plasmonics in semiconductor heterostructures and graphene have been the subject of considerable interest in the field of research.^{1–6} It has been receiving increasing attention partly due to lacking technological development in the terahertz (THz) frequency range (0.1 – 10 THz) used in a number of devices.^{7,8} These include ultrasensitive plasmonic detectors,^{9–15} spectrometers,^{16,17} and generators.^{18–21}

A critical advantage of plasmonic devices is the tunability of their parameters accomplished by changing the density in a two-dimensional electron system (2DES). Recently, a new application of plasmonic devices in the area of THz phase shifting and modulation has been theoretically proposed.^{22–27} An active array of such phase modulators can play a significant role in applications involving beam steering and programmable holographic projections, ultimately aimed at developing THz communication systems. Recent experiments on AlGaAs/GaAs semiconductor heterostructures have shown that a bare 2D layer of electrons can efficiently tune the phase of the penetrating electromagnetic radiation.²⁸ Indeed, the 2DES impedance is well described by the Drude model as follows:^{29–33}

$$Z_{2DES}(\omega) = R + i\omega L_K, \quad L_K = \frac{m^*}{n_s e^2}. \quad (1)$$

Here, $R = m^*/n_s e^2 \tau$ is the resistance per square unit area of the 2DES, m^* is the effective mass, n_s is the 2DES electron density, τ is the relaxation time, and L_K is the kinetic inductance arising from the collective motion of 2D electrons. Provided that $\omega L_K \gg R$, which is equivalent

to $\omega\tau \gg 1$, the two-dimensional electron layer acts as 2D plasma. In this plasmonic regime, the phase shift in the radiation passing through the 2DES can be expressed as (see the supplementary material for details)

$$\Delta\phi = \arctan \frac{Z_0/2\omega L_K}{1 + \left(1 + \frac{Z_0}{2R}\right) \frac{1}{\omega^2 \tau^2}}, \quad (2)$$

where $Z_0 = \sqrt{\mu_0/\epsilon_0} = 377 \Omega$ is the vacuum impedance, which, in Gaussian units, can be expressed as $Z_0 = 1$. We note that the inductive reactance, ωL_K , can be tuned either by adjusting the 2DES electron density, n_s , or by applying an external magnetic-field perpendicular to the 2DES plane.

Unfortunately, all 2DES-based plasmonic devices suffer from severe degradation in their performance with increasing temperature. However, there is not much experimental data on the temperature effects on the performance deterioration in plasmonic THz devices. In the present paper, we study the temperature degradation of the phase shift $\Delta\phi$ introduced by the two-dimensional layer. We find the relationship (2) to be in good agreement with the experimental results, indicating the dominant role of the $\omega\tau$ factor in the relaxation of the 2D plasma. We demonstrate that at frequencies above 300 GHz, the GaAs semiconductor phase modulator can operate at up to room temperature with virtually no degeneration in its performance. These findings open up exciting possibilities for the practical application of the developed plasmonic technology.

Experiments have been performed on a $\text{Al}_{0.3}\text{Ga}_{0.7}\text{As}/\text{GaAs}/\text{Al}_{0.3}\text{Ga}_{0.7}\text{As}$ heterostructure grown by molecular beam epitaxy. The first industrial wafer has a 20 nm quantum well located at a distance of 210 nm below the crystal surface. The 2DES electron density in the quantum well was $n_s = 1.3 \times 10^{12} \text{ cm}^{-2}$ with low-temperature mobility of around $10^5 \text{ cm}^2/\text{V s}$ ($T = 5 \text{ K}$) and room temperature mobility of $9000 \text{ cm}^2/\text{V s}$ ($T = 300 \text{ K}$). A $1 \times 1 \text{ cm}^2$ sample is mounted on a sample holder with an 8 mm pinhole at the location of the sample. The entire arrangement is oriented in the Faraday geometry inside an optical cryostat, with a split-coil providing the magnetic field of up to $\pm 7 \text{ T}$ applied perpendicular to the sample surface. Continuous monochromatic radiation is generated by backward-wave oscillators operating in the submillimeter frequency range of 20–600 GHz. The phase of the electromagnetic wave transmitted through the 2DES is measured using the Mach–Zehnder interferometric method.^{28,34} In this technique, the interferometer is set to operate in such a way that during the magnetic-field sweep, the mobile mirror in the reference arm is constantly moving to maintain the interferometer in a balanced state, with zero signal on the detector. The phase shift is then calculated according to the measured displacement in the mirror position [Fig. 1(a)].

To determine the phase shift, $\Delta\phi$, introduced by the 2DES, we rely on applying the external magnetic field.³⁵ When the applied magnetic field is strong, i.e., $\omega_c\tau = (eB/m^*)\tau \gg 1$ and $\omega_c \gg \omega$, it quenches the 2D plasma motion, leading to the unitary transmission through the 2DES. Indeed, in the presence of the magnetic field, the transmission and reflection from the 2DES can be expressed as³⁶

$$\begin{aligned} Tr &= |t|^2 = 1 - \frac{\Gamma^2 + 2\gamma\Gamma}{(\omega - \omega_c)^2 + (\gamma + \Gamma)^2}, \\ R &= \frac{\Gamma^2}{(\omega - \omega_c)^2 + (\gamma + \Gamma)^2}, \\ \Gamma &= \frac{n_s e^2}{2\epsilon_0 m^* c} \quad \gamma = \frac{1}{\tau}. \end{aligned} \quad (3)$$

Therefore, since the 2D electron layer does not contribute to the phase shift at $Tr(B \rightarrow \infty) = 1$, we arrive at $\Delta\phi = \phi(4 \text{ T}) - \phi(0 \text{ T})$ for the given data. As was mentioned earlier, the phase shift can also be tuned electronically by sweeping the gate voltage,²⁸ which is generally preferred in device applications. In the present investigation, however, the magnetic-field sweep is chosen as a matter of convenience. Regardless of a particular choice, both approaches give the same result.

Figure 1(b) shows the dependence of $\Delta\phi$ on frequency. In order to eliminate the effect of the semiconductor substrate, the measurements are taken at the Fabry–Pérot resonance frequencies: $\omega_N = N\omega_d = N\pi/\sqrt{\epsilon d}$ ($N = 1, 2, 3, \dots$), where ϵ is the dielectric permittivity of the substrate and d is its thickness.³⁷ In this case, the sample with $d = 0.62 \text{ mm}$ and $n_s = 1.3 \times 10^{12} \text{ cm}^{-2}$ is measured at $T = 5 \text{ K}$. In the figure, the measurement data (red dots) are compared to the theoretical prediction (2) in the limit of $\omega\tau \gg 1$. The resulting dependence $\Delta\phi = \arctan(Z_0/2\omega L_K)$ is in good agreement with experimental results.

One of the crucial questions on the way to the practical application of the developed phase shifter is whether it can be used at room temperature. It follows from Eq. (2) that it is, indeed, possible, provided that $\omega\tau > 1$. Figure 2(a) shows $\Delta\phi$ as a function of temperature T , measured at 139 and 410 GHz. At these radiation frequencies, we

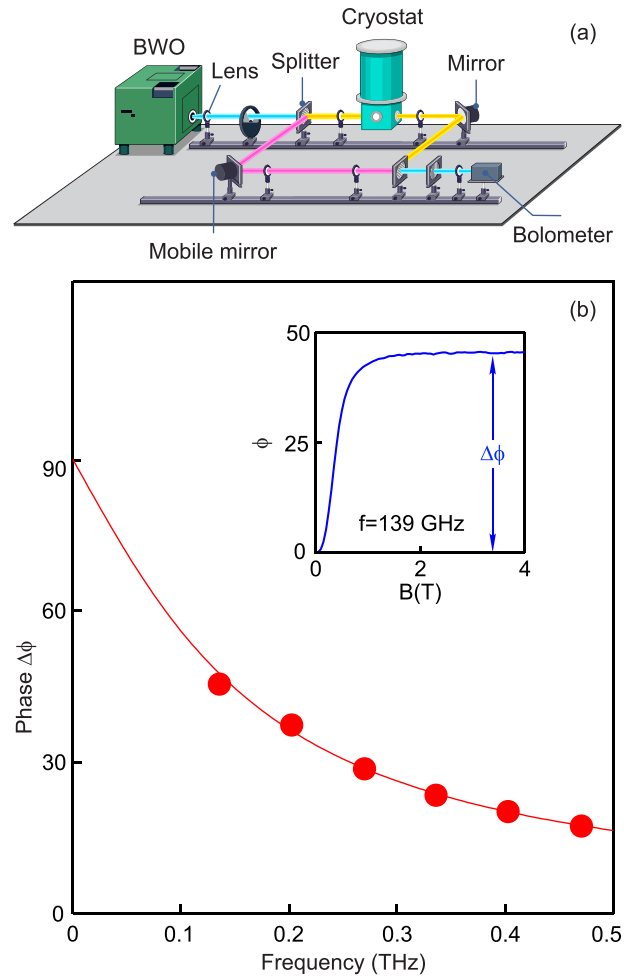


FIG. 1. (a) Schematic diagram of the Mach–Zehnder interferometric setup. (b) The phase shift $\Delta\phi$ vs the Fabry–Pérot resonance frequency f_N , measured for the 2DES with $n_s = 1.3 \times 10^{12} \text{ cm}^{-2}$ at $T = 5 \text{ K}$ (red dots). The solid line is the theoretical prediction according to $\Delta\phi = \arctan(Z_0/2\omega L_K)$. The left inset shows the transmission-line model of the device under study. The right inset shows the magnetic-field dependence of the phase of the electromagnetic wave transmitted through the 2DES at $f = 139 \text{ GHz}$.

obtain $\Delta\phi = 46.8^\circ$ and 15.6° at a temperature of 5 K. For better visual comparison, we plot the two datasets normalized to the phase shift at $T = 5 \text{ K}$. The graphs make it evident that with increasing frequency, the degradation of the phase shifter performance becomes less prominent. Most importantly, the data demonstrate that at 410 GHz, the device can operate at temperatures as high as 300 K (room temperature). In this case, the phase of the electromagnetic radiation is tuned by the magnetic field in the range of $\Delta\phi = 7^\circ$.

To compare the experimental data with the quantitative description of the temperature effect, Fig. 2(a) includes the predictions calculated from (2) plotted in solid lines. The effective mass m^* and the relaxation time τ are determined from the B -field position and line width of the cyclotron resonance observed in transmission. There is a good agreement between the experimental data and theory. In the

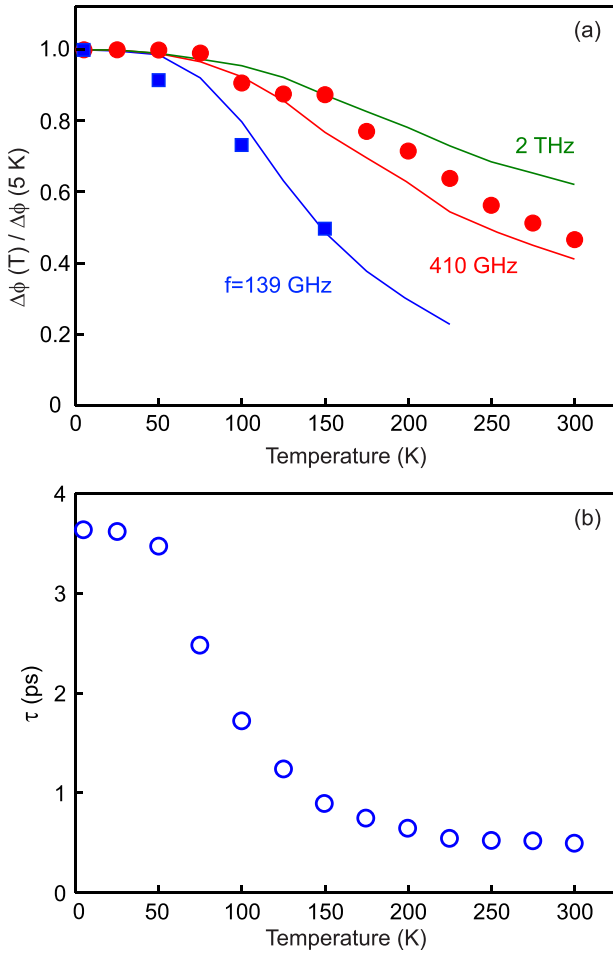


FIG. 2. (a) Dependence of the phase shift $\Delta\phi$ on the temperature T measured at $f=139\text{ GHz}$ (blue squares) and $f=410\text{ GHz}$ (red dots). The solid lines indicate the theoretical predictions according to Eq. (2). Experimental data for 410 GHz prove a successful operation of the device up to room temperature. (b) The plot of the relaxation time, τ , vs temperature. At room temperature, the plasma condition $\omega\tau > 1$ is satisfied when $f > 1/(2\pi\tau) \approx 300\text{ GHz}$.

same figure, we additionally plot the expected behavior of $\Delta\phi$ vs temperature calculated for $f=2\text{ THz}$ (green line) to illustrate the general trend over higher frequencies. The resultant temperature dependence of the relaxation time is plotted in Fig. 2(b), indicating that $\tau = 0.5\text{ ps}$ at room temperature. Therefore, to fulfill the plasma condition $\omega\tau > 1$, it is required to have $f > 1/(2\pi\tau) \approx 300\text{ GHz}$. It is the critical frequency above which the response of the 2DES to the electromagnetic radiation becomes plasmonic at room temperature. It is interesting to understand what determines phase degradation at frequencies above 300 GHz.

Figure 3(a) shows the magnetic-field sweeps recorded for $f=410\text{ GHz}$ at the temperatures of 5, 150, and 250 K, with a well-resolved cyclotron resonance (CR) observed at $\omega_c = eB/m^*$. Importantly, we clearly see that the cyclotron resonance shifts to larger magnetic fields with rising temperature. It indicates a substantial increase in the effective mass of charge carriers (m^*) shown in detail in

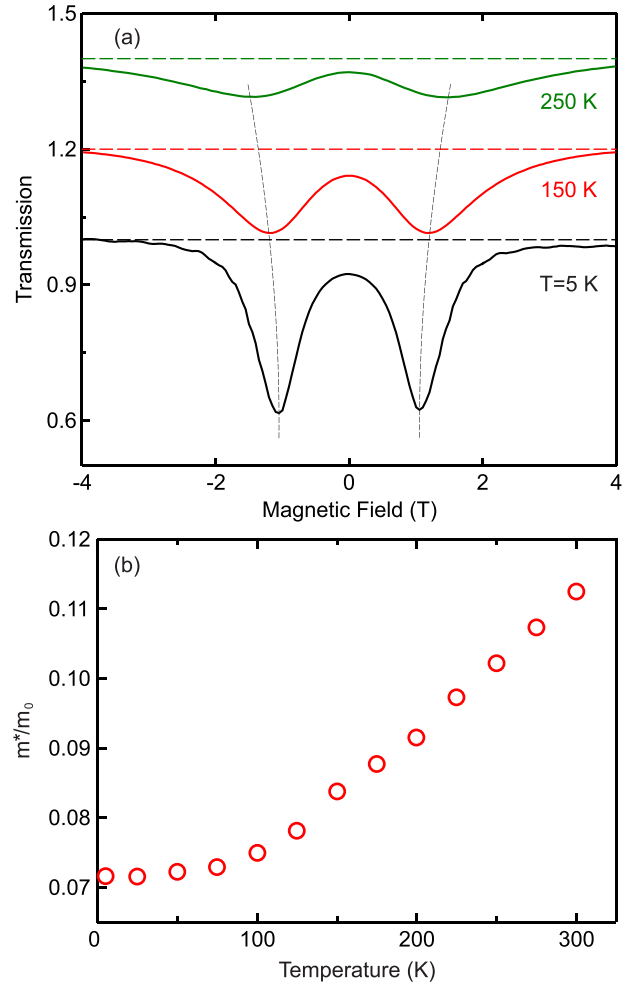


FIG. 3. (a) Magnetic-field sweeps of transmission measured for $f=410\text{ GHz}$ at three different temperatures T . The transmission curves for $T=150$ and 250 K have been shifted vertically by 0.2 and 0.4, respectively. The dashed lines for each of the curves show the level of total transmittance. The data show that CR resonance shifts to larger magnetic fields as the temperature increases. (b) Dependence of the effective mass m^* on temperature measured for the GaAs/AlGaAs 2DES with $n_s = 1.3 \times 10^{12}\text{ cm}^{-2}$.

Figure 3(b). A similar effect has been reported in AlGaIn/GaN heterostructures.^{38,39} Part of the change in mass with increasing temperature is due to the effects of band non-parabolicity. Indeed, the two-dimensional electrons form a Fermi sphere with Fermi energy of $E_f=46\text{ meV}$. This results in an increase in mass from the GaAs band value of $0.067 m_0$ to $0.072 m_0$ observed in the experiment. The room temperature 300 K corresponds to the non-degenerate electron energy of 26 meV. Therefore, non-parabolicity effects can only explain the change in mass of $\Delta m^* = 0.003 m_0$. This is a minor part of the discovered change in mass $\Delta m^* = 0.026 m_0$.

Although the physical origin of the observed drastic change in effective mass is not clear at the moment, it has been suggested that it might be related to the interaction between electrons and optical phonons,⁴⁰ or to a change in spatial confinement of two-dimensional

electron gas at room temperature.³⁸ We can see in Fig. 2(a) that the temperature dependency of $\Delta\phi$ does not significantly differ between 410 GHz and 2 THz. This result indicates that the main factor in $\Delta\phi$ degradation above 300 GHz is not related to the plasma parameter $\omega\tau$, but rather to the increase of the effective mass. This phenomenon should be given due consideration in the practical design of plasmonic devices.

In conclusion, we have investigated the operation of the plasmonic phase shifter at different temperatures. We have found the temperature-dependent change in the relaxation time and effective mass to be the major factor contributing to the degradation of the phase shifter performance. The CR spectroscopy experiments reveal an unexpectedly large change in the effective mass with increasing temperature. Importantly, experiments demonstrate that above 300 GHz, the phase shifter can operate at up to room temperature. These findings pave the way to the plasmonic phase-shifting technology in a range of beam steering applications.

See the supplementary material for the derivation of the phase shift in electromagnetic radiation passing through a 2DES.

The authors gratefully acknowledge the financial support from the Russian Science Foundation (Grant No. 19-72-30003).

AUTHOR DECLARATIONS

Conflict of Interest

The authors have no conflicts to disclose.

Author Contributions

Kirill R. Dzhikirba: Conceptualization (equal); Data curation (equal); Formal analysis (equal); Funding acquisition (equal); Investigation (equal); Methodology (equal); Project administration (equal); Resources (equal); Software (equal); Supervision (equal); Validation (equal); Visualization (equal); Writing – original draft (equal); Writing – review & editing (equal). **Alexey Shuvaev:** Conceptualization (equal); Data curation (equal); Formal analysis (equal); Funding acquisition (equal); Investigation (equal); Methodology (equal); Project administration (equal); Resources (equal); Software (equal); Supervision (equal); Validation (equal); Visualization (equal); Writing – original draft (equal); Writing – review & editing (equal). **Daniyar A. Khudaiberdiev:** Conceptualization (equal); Data curation (equal); Formal analysis (equal); Funding acquisition (equal); Investigation (equal); Methodology (equal); Project administration (equal); Resources (equal); Software (equal); Supervision (equal); Validation (equal); Visualization (equal); Writing – original draft (equal); Writing – review & editing (equal). **Igor Kukushkin:** Conceptualization (equal); Data curation (equal); Formal analysis (equal); Funding acquisition (equal); Investigation (equal); Methodology (equal); Project administration (equal); Resources (equal); Software (equal); Supervision (equal); Validation (equal); Visualization (equal); Writing – original draft (equal); Writing – review & editing (equal). **Viacheslav Mihailovich Muravev:** Conceptualization (equal); Data curation (equal); Formal analysis (equal); Funding acquisition (equal); Investigation (equal); Methodology (equal); Project administration (equal); Resources (equal); Software (equal); Supervision (equal); Validation (equal); Visualization (equal); Writing – original draft (equal); Writing – review & editing (equal).

DATA AVAILABILITY

The data that support the findings of this study are available from the corresponding author upon reasonable request.

REFERENCES

- D. Heitmann, *Surf. Sci.* **170**, 332 (1986).
- S. A. Mikhailov, *Phys. Rev. B* **70**, 165311 (2004).
- F. H. L. Koppens, D. E. Chang, and F. J. García de Abajo, *Nano Lett.* **11**, 3370 (2011).
- D. N. Basov, M. M. Fogler, and F. J. García de Abajo, *Science* **354**, 195 (2016).
- J. Lusakowski, *Semicond. Sci. Technol.* **32**, 013004 (2016).
- V. M. Muravev and I. V. Kukushkin, *Phys.-Usp.* **63**(10), 975 (2020).
- Y.-S. Lee, *Principles of Terahertz Science and Technology* (Springer Science & Business Media, 2009), Vol. 170.
- Z. Xi-Cheng and J. Xu, *Introduction to THz Wave Photonics* (Springer, New York, 2010), Vol. 29.
- W. Knap, Y. Deng, S. Romyantsev, and M. S. Shur, *Appl. Phys. Lett.* **81**, 4637 (2002).
- E. A. Shaner, M. Lee, M. C. Wanke, A. D. Grine, J. L. Reno, and S. J. Allen, *Appl. Phys. Lett.* **87**, 193507 (2005).
- V. V. Popov, D. V. Fateev, T. Otsuji, Y. M. Meziani, D. Coquillat, and W. Knap, *Appl. Phys. Lett.* **99**, 243504 (2011).
- L. Vicarelli, M. S. Vitiello, D. Coquillat, A. Lombardo, A. C. Ferrari, W. Knap, M. Polini, V. Pellegrini, and A. Tredicucci, *Nat. Mater.* **11**, 865 (2012).
- V. M. Muravev and I. V. Kukushkin, *Appl. Phys. Lett.* **100**, 082102 (2012).
- D. Spirito, D. Coquillat, S. L. De Bonis, A. Lombardo, M. Bruna, A. C. Ferrari, V. Pellegrini, A. Tredicucci, W. Knap, and M. S. Vitiello, *Appl. Phys. Lett.* **104**, 061111 (2014).
- X. Cai, A. B. Sushkov, R. J. Suess, M. M. Jadidi, G. S. Jenkins, L. O. Nyakiti, R. L. Myers-Ward, S. Li, J. Yan, D. K. Gaskill, T. E. Murphy, H. D. Drew, and M. S. Fuhrer, *Nat. Nanotechnol.* **9**, 814 (2014).
- V. M. Muravev, A. A. Fortunatov, A. A. Dremin, and I. V. Kukushkin, *JETP Lett.* **103**, 380 (2016).
- D. A. Bandurin, D. Svintsov, I. Gayduchenko, S. G. Xu, A. Principi, M. Moskotin, I. Tretiyakov, D. Yagodkin, S. Zhukov, T. Taniguchi, K. Watanabe, I. V. Grigorieva, M. Polini, G. N. Goltsman, A. K. Geim, and G. Fedorov, *Nat. Commun.* **9**, 5392 (2018).
- W. Knap, J. Lusakowski, T. Parenty, S. Bollaert, A. Cappy, V. V. Popov, and M. S. Shur, *Appl. Phys. Lett.* **84**(13), 2331 (2004).
- N. Dyakonova, A. E. Fatimy, J. Lusakowski, W. Knap, M. I. Dyakonov, M.-A. Poisson, E. Morvan, S. Bollaert, A. Shchepetov, Y. Roelens, C. Gaquiere, D. Theron, and A. Cappy, *Appl. Phys. Lett.* **88**(14), 141906 (2006).
- O. Sidoruk, R. R. A. Syms, and L. Solymar, *Opt. Express* **20**, 19618 (2012).
- H. A. Hafez, S. Kovalev, J.-C. Deinert, Z. Mics, B. Green, N. Awari, M. Chen, S. Germanskiy, U. Lehnert, J. Teichert, Z. Wang, K.-J. Tielrooij, Z. Liu, Z. Chen, A. Narita, K. Müllen, M. Bonn, M. Gensch, and D. Turchinovich, *Nature* **561**, 507 (2018).
- F. Lu, B. Liu, and S. Shen, *Adv. Opt. Mater.* **2**(8), 794–799 (2014).
- E. Carrasco, M. Tamagnone, J. R. Mosig, T. Low, and J. Perruisseau-Carrier, *Nanotechnology* **26**(13), 134002 (2015).
- Z. Li, K. Yao, F. Xia, S. Shen, J. Tian, and Y. Liu, *Sci. Rep.* **5**(1), 12423 (2015).
- T. Yatooshi, A. Ishikawa, and K. Tsuruta, *Appl. Phys. Lett.* **107**(5), 053105 (2015).
- S. R. Biswas, C. E. Gutiérrez, A. Nemilentsau, I. H. Lee, S. H. Oh, P. Avouris, and T. Low, *Phys. Rev. Appl.* **9**(3), 034021 (2018).
- X. Shang, L. Xu, H. Yang, H. He, Q. He, Y. Huang, and L. Wang, *New J. Phys.* **22**(6), 063054 (2020).
- V. M. Muravev, A. Shuvaev, A. S. Astrakhantseva, P. A. Gusikhin, I. V. Kukushkin, and A. Pimenov, *Appl. Phys. Lett.* **121**, 051101 (2022).
- P. J. Burke, I. B. Spielman, J. P. Eisenstein, L. N. Pfeiffer, and K. W. West, *Appl. Phys. Lett.* **76**, 745 (2000).
- G. C. Dyer, G. R. Aizin, S. J. Allen, A. D. Grine, D. Bethke, J. L. Reno, and E. A. Shaner, *Nat. Photonics* **7**, 925 (2013).
- H. Yoon, K. Yeung, P. Kim, and D. Ham, *Philos. Trans. R. Soc. A* **372**, 20130104 (2014).

- ³²H. Yoon, C. Forsythe, L. Wang, N. Tombros, K. Watanabe, T. Taniguchi, J. Hone, P. Kim, and D. Ham, *Nat. Nanotechnol.* **9**, 594 (2014).
- ³³V. M. Muravev, N. D. Semenov, I. V. Andreev, P. A. Gusikhin, and I. V. Kukushkin, *Appl. Phys. Lett.* **117**, 151103 (2020).
- ³⁴G. Kozlov and A. Volkov, *Topics in Applied Physics*, edited by G. Grüner, Millimeter and Submillimeter Wave Spectroscopy of Solids (Springer-Verlag Berlin-Heidelberg, 1998), Vol. 74.
- ³⁵V. M. Muravev, A. V. Shchepetilnikov, K. R. Dzhikirba, I. V. Kukushkin, R. Schott, E. Cheah, W. Wegscheider, and A. Shuvaev, *Phys. Rev. Appl.* **19**, 024039 (2023).
- ³⁶K. W. Chiu, T. K. Lee, and J. J. Quinn, *Surf. Sci.* **58**, 182 (1976).
- ³⁷M. Dressel and G. Grüner, *Electrodynamics of Solids: Optical Properties of Electrons in Matter*, 1st ed. (Cambridge University Press, 2003).
- ³⁸T. Hofmann, P. Kuhne, S. Schoche, J.-T. Chen, U. Forsberg, E. Janzen, N. Ben Sedrine, C. M. Herzinger, J. A. Woollam, M. Schubert, and V. Darakchieva, *Appl. Phys. Lett.* **101**, 192102 (2012).
- ³⁹D. Pashnev, V. V. Korotyeyev, J. Jorudas, T. Kaplas, V. Janonis, A. Urbanowicz, and I. Kašalynasa, *Appl. Phys. Lett.* **117**, 162101 (2020).
- ⁴⁰V. V. Korotyeyeva, V. A. Kochelap, V. V. Kaliuzhnyi, and A. E. Belyaev, *Appl. Phys. Lett.* **120**, 252103 (2022).